Inorganic Chemistry
ARTICLE
pubs.acs.org/IC

How Does the Nickel Pincer Complex Catalyze the Conversion of CO_2 to a Methanol Derivative? A Computational Mechanistic Study

Fang Huang,[†] Chenggen Zhang,[†] Jinliang Jiang,[†] Zhi-Xiang Wang,[*,†] and Hairong Guan[*,‡]

[†]College of Chemistry and Chemical Engineering, Graduate University of the Chinese Academy of Sciences, Beijing, 100049, China
[‡]Department of Chemistry, University of Cincinnati, P.O. Box 21072, Cincinnati, Ohio 45221-0172, United States

Supporting Information

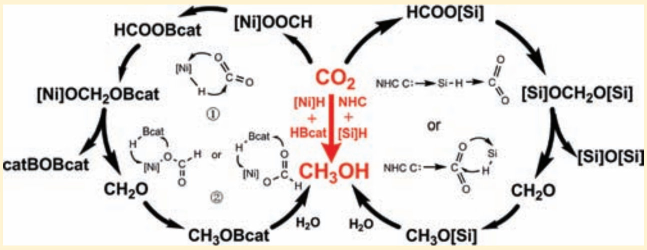

ABSTRACT: The mechanistic details of nickel-catalyzed reduction of CO_2 with catecholborane (HBcat) have been studied by DFT calculations. The nickel pincer hydride complex ({2,6-$C_6H_3(OP^tBu_2)_2$}NiH = [Ni]H) has been shown to catalyze the sequential reduction from CO_2 to HCOOBcat, then to CH_2O, and finally to CH_3OBcat. Each process is accomplished by a two-step sequence at the nickel center: the insertion of a C═O bond into [Ni]H, followed by the reaction of the insertion product with HBcat. Calculations have predicted the difficulties of observing the possible intermediates such as [Ni]OCH_2OBcat, [Ni]OBcat, and [Ni]OCH_3, based on the low kinetic barriers and favorable thermodynamics for the decomposition of [Ni]OCH_2OBcat, as well as the reactions of [Ni]OBcat and [Ni]OCH_3 with HBcat. Compared to the uncatalyzed reactions of HBcat with CO_2, HCOOBcat, and CH_2O, the nickel hydride catalyst accelerates the $H^{\delta-}$ transfer by lowering the barriers by 30.1, 12.4, and 19.6 kcal/mol, respectively. In general, the catalytic role of the nickel hydride is similar to that of *N*-heterocyclic carbene (NHC) catalyst in the hydrosilylation of CO_2. However, the $H^{\delta-}$ transfer mechanisms used by the two catalysts are completely different. The $H^{\delta-}$ transfer catalyzed by [Ni]H can be described as hydrogen being shuttled from HBcat to nickel center and then to the C═O bond, and the catalyst changes its integrity during catalysis. In contrast, the NHC catalyst simply exerts an electronic influence to activate either the silane or CO_2, and the integrity of the catalyst remains intact throughout the catalytic cycle. The comparison between [Ni]H and $Cp_2Zr(H)Cl$ in the stoichiometric reduction of CO_2 has suggested that ligand sterics and metal electronic properties play critical roles in controlling the outcome of the reaction. A bridging methylene diolate complex has been previously observed in the zirconium system, whereas the analogous [Ni]OCH_2O[Ni] is not a viable intermediate, both kinetically and thermodynamically. Replacing HBcat with $PhSiH_3$ in the nickel-catalyzed reduction of CO_2 results in a high kinetic barrier for the reaction of [Ni]OOCH with $PhSiH_3$. Switching silanes to HBcat in NHC-catalyzed reduction of CO_2 generates a very stable NHC adduct of HCOOBcat, which makes the release of NHC less favorable.

1. INTRODUCTION

Excessive use of fossil fuels has significantly raised the CO_2 concentration in the atmosphere, which is one of the leading factors in global warming. On the other hand, CO_2 can serve as an abundant and inexpensive carbon source for the synthesis of value-added chemicals.[1,2] Among many catalytic processes involving CO_2, its reduction to CH_4,[3] CH_3OH,[4] HCOOH,[5−7] or CO[8−10] promoted by homogeneous transition-metal complexes is a promising way to utilize this specific greenhouse gas. For practical applications, the conversion CO_2 to CH_3OH is particularly attractive, because of the convenience in transporting and storing a liquid fuel. Floriani and co-workers have reported that $Cp_2Zr(H)Cl$, which is an early-transition-metal complex, can be used to mediate the stoichiometric conversion of CO_2 to CH_3OH.[4g,h] Sasaki and co-workers have shown a catalytic system that uses $Ru_3(CO)_{12}$-KI to promote the hydrogenation of CO_2 to a mixture of CH_4, CH_3OH, and CO.[4f] Eisenschmid and Eisenberg demonstrated that Ir(CN)(CO)(dppe) [dppe = 1,2-bis(diphenylphosphino)ethane] is a viable catalyst for the hydrosilylation of CO_2 to the methoxide level.[4i] Recently, transition-metal-free systems such as TMP/$B(C_6F_5)_3/H_2$ (reported by the Ashley and O'Hare groups[4c]) and $PMe_3/AlX_3/NH_3BH_3$ (reported by the Stephan group[4b]) have also been used to achieve the reduction of CO_2. Computationally, Chan and Radom have examined the strategies of using zeolite catalysts to convert CO_2 to methanol.[4d,e]

Recently, Zhang et al. have reported organocatalytic transformation of CO_2 into CH_3OH derivatives using an *N*-heterocyclic carbene (NHC) as the catalyst and silanes (R_3SiH = [Si]H) as the reducing reagents (termed as NHC/CO_2/silane system).[11] One of us has reported the catalytic conversion of CO_2 to a methoxy boron compound, using a nickel pincer hydride complex ({2,6-C_6H_3-$(OP^tBu_2)_2$}NiH = [Ni]H) as the catalyst and catecholborane

Received: February 1, 2011
Published: March 17, 2011

Scheme 1. Comparison between [Ni]H- and NHC-Catalyzed CO_2 Reduction Reactions[a]

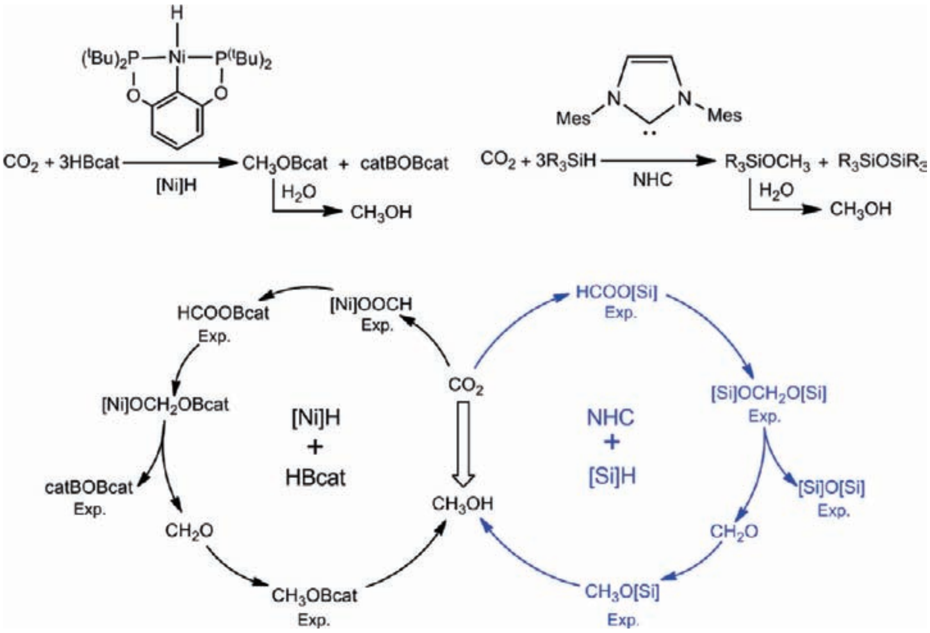

[a] "Exp." denotes experimentally observed species.

(HBcat) as the hydrogen source (termed as the $[Ni]H/CO_2/HBcat$ system).[12] Close examination of the experimental details of these two systems, as summarized in Scheme 1, has revealed some interesting similarities. First of all, both systems use 3 equiv of hydrogen sources to reduce 1 equiv of CO_2. Second, in terms of experimentally detected species, there are several one-to-one correlations (i.e., HCOOBcat ↔ HCOO[Si], catBOBcat ↔ [Si]O[Si], and CH_3OBcat ↔ $CH_3O[Si]$). In addition, CH_2O has been proposed as an important intermediate in the catalytic cycle of $[Ni]H/CO_2/HBcat$ system.[12] Our previous study of the NHC/CO_2/silane system has showed that CH_2O is also an inevitable intermediate,[13] although it has not been reported in the experimental study.[11] There are also several differences in these two catalytic systems. For example, $[Si]OCH_2O[Si]$ has been detected in the NHC/CO_2/silane system, whereas $catBOCH_2OBcat$ has not been observed. While [Ni]OOCH has been found in the $[Ni]H/CO_2/HBcat$ system, the counterpart in the NHC/CO_2/silane system remains elusive. Furthermore, unlike the NHC/CO_2/silane system, where the NHC catalyst has been shown to participate in three $H^{\delta-}$ transfer steps, the [Ni]H catalyst has been proposed to promote two $H^{\delta-}$ transfer steps, with the second $H^{\delta-}$ transfer step (HCOOBcat + HBcat → CH_2O + catBOBcat) being left uncatalyzed. To further understand these two catalytic systems, we have performed a detailed computational study to gain the mechanistic insights into Ni-catalyzed reduction of CO_2 with HBcat. We have compared the results with our previously investigated NHC/CO_2/silane catalytic system, as well as the stoichiometric reduction of CO_2 mediated by other transition-metal hydride complexes.

2. COMPUTATIONAL DETAILS

Calculations throughout this paper were performed on the full structures of the reported compounds, rather than their truncated models. All the structures were optimized and characterized as minima or transition states at the B3LYP[14]/BSI level (BSI designates the basis set with a combination of LanL2DZ[15] for Ni and 6-31G* for all nonmetal atoms) in the gas phase. At the B3LYP/BSI structures, the energies were then refined by the B3LYP/6-31+G** (i.e., 6-31+G** basis set used for all atoms, including Ni) single-point calculations with the solvation effects of toluene (experimentally used) included and simulated by IEFPCM[16] solvent model. The gas-phase B3LYP/BSI frequencies were used for thermal and entropic corrections at 298.15 K and 1 atm. The free energies are discussed, unless otherwise specified, and the enthalpies are given for reference. Natural bond orbital (NBO)[17] analyses were performed at the B3LYP/6-31+G** level to assign the atomic charges (*Q*) and to measure the Wiberg bond indices (WBI). The suitability of single-point energy refinements at the structures optimized using the relatively small BSI basis set was examined. We selected some stationary points and reoptimized them at the B3LYP/6-31+G** level. The energetic results from these optimization calculations agree with the B3LYP/6-31+G**//B3LYP/BSI values within a deviation of <0.4 kcal/mol (see section SI1 in the Supporting Information). Meanwhile, for these representative stationary points, the B3LYP/6-31+G**//B3LYP/BSI relative energies were examined in comparison with the B3LYP/6-311++G**//B3LYP/BSI values; they are in reasonable agreement with each other (see section SI1 in the Supporting Information). All the optimized structures involved in this study are given in section SI2 in the Supporting Information. In the main text, we only present the optimized

Scheme 2. Proposed Mechanism for the Catalytic Conversion of CO_2 to CH_3OBcat

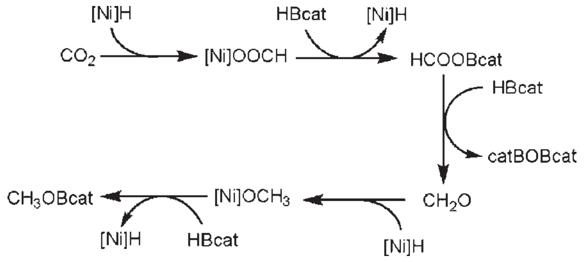

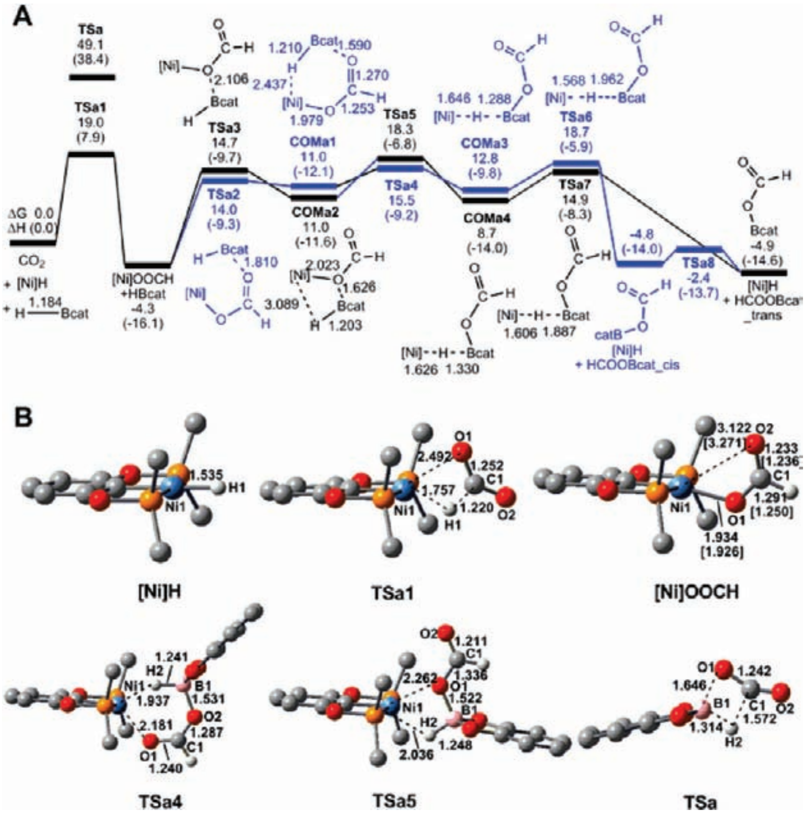

Figure 1. (A) Free-energy profile of HCOOBcat formation steps (values given in kcal/mol; the enthalpy values are listed in the parentheses). The key bond lengths in the stationary points are given in Ångstroms. (B) Optimized structures of important stationary points with key bond lengths (given in Ångstroms). Optimized structures of other stationary points are given in section SI2 in the Supporting Information. The bond lengths of [Ni]OOCH (given in the brackets) are based on X-ray data. Trivial H atoms and the methyl groups on the pincer ligand of [Ni]H are omitted for the sake of clarity.

structures of important stationary points. All calculations were carried out using Gaussian 03.[18]

3. RESULTS AND DISCUSSION

3.1. Overall Catalytic Mechanism. In the experimental study of the [Ni]H/CO_2/HBcat system, intermediate [Ni]OOCH and HCOOBcat were identified, along with the two products CH_3OBcat and catBOBcat.[12] A mechanism including all these species was proposed and depicted in Scheme 2. Although CH_2O was not detected experimentally, it was postulated to be generated via the reaction of HCOOBcat with HBcat. Our calculations show that CH_2O is indeed an important intermediate; however, its formation from HCOOBcat is catalyzed by [Ni]H (vide infra). In the following sections, we describe our computational results following the proposed reaction segments in Scheme 2.

Formation of HCOOBcat. Figure 1A illustrates the reaction pathways for the formation of HCOOBcat, which involves the initial CO_2 insertion into the Ni−H bond of [Ni]H via the transition state **TSa1**, followed by the interaction of [Ni]OOCH with 1 equiv of HBcat. The insertion of CO_2 into a metal hydride complex is often the first elemental step in transition-metal-catalyzed hydrogenation of CO_2 to HCOOH, and its mechanistic details are well understood.[7] For a related nickel PCP-pincer system [PCP = 2,6-$C_6H_3(CH_2P^tBu_2)_2$], Hazari et al. have studied the insertion of CO_2 into Ni−R (R = H, Me, and allyl) bonds.[19] In the present case, CO_2 insertion crosses a barrier of 19.0 kcal/mol (**TSa1**) and is exergonic by 4.3 kcal/mol. The low barrier and small exergonicity are consistent with the experimental observation that the insertion reaction is rapid and reversible at ambient temperature. The computed enthalpy (24.0 kcal/mol) for the decarboxylation of [Ni]OOCH, the reverse step of CO_2 insertion, is also in accordance with the experimentally determined value (21.6 ± 1.1 kcal/mol).[20] Furthermore, the optimized structure of [Ni]OOCH is in reasonable agreement with the X-ray data (see [Ni]OOCH in Figure 1B), supporting the suitability of the employed computational method.

The insertion product [Ni]OOCH reacts with HBcat (the first equivalent of HBcat used in a complete catalytic cycle) to give the experimentally detected HCOOBcat and regenerate the [Ni]H catalyst. As shown in the schematic structures of the transition states **TSa2** and **TSa3**, the electron-deficient B atom of HBcat attacks either of the O atoms of [Ni]OOCH via a donor−acceptor interaction, which creates two independent pathways (see Figure 1A). After crossing **TSa2** or **TSa3**, the attack of HBcat first leads to a six-membered (**COMa1**) or a four-membered donor−acceptor complex (**COMa2**). The $H^{\delta-}$ of HBcat moiety in the complex is then transferred to the Ni center of [Ni]OOCH by crossing the transition states **TSa4** or **TSa5**, forming a H-bridged complex (**COMa3** or **COMa4**). The dissociation of the H-bridged complex produces HCOOBcat and regenerates the [Ni]H catalyst after crossing the transition state **TSa6** or **TSa7**. The transition states for HCOOBcat dissociation (**TSa6**) and $H^{\delta-}$ transfer (**TSa5**) are the highest stationary points on the

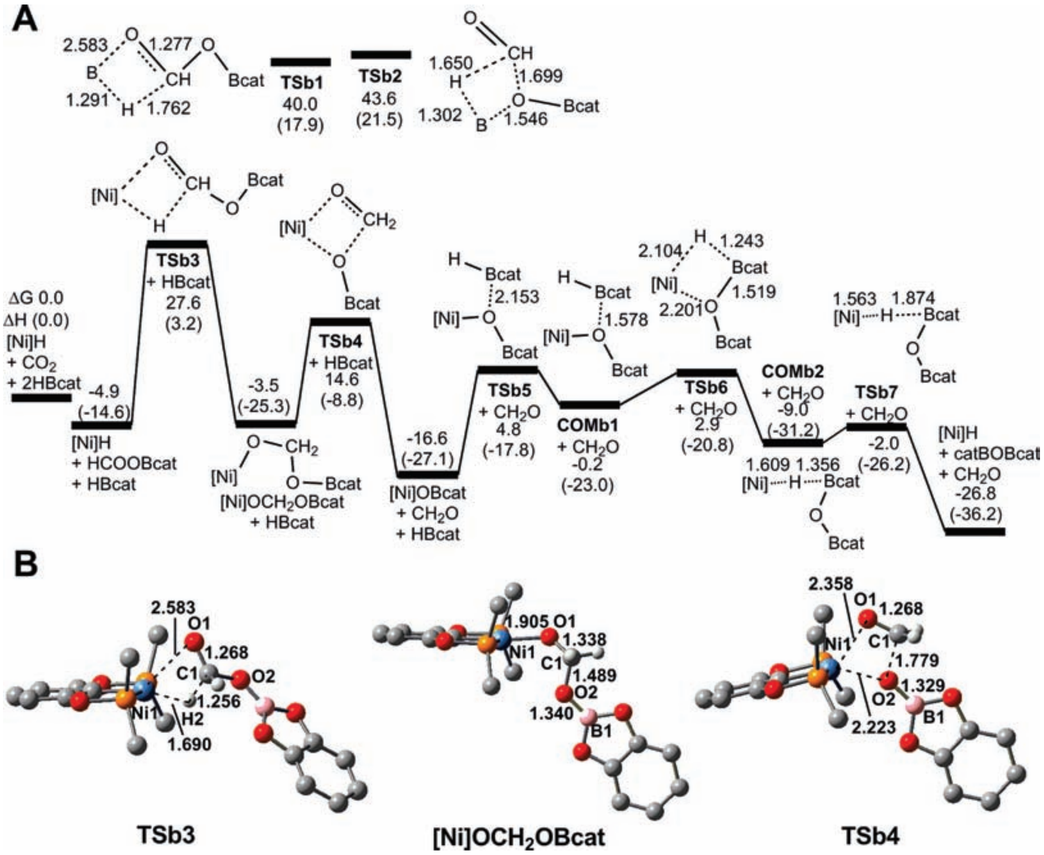

Figure 2. (A) Free-energy profile of CH_2O formation steps (values in kcal/mol; the enthalpy values are listed in the parentheses). The key bond lengths in the stationary points are given in Ångstroms. (B) Optimized structures of important stationary points with key bond lengths (given in Ångstroms). Other optimized structures are given in section SI2 in the Supporting Information. Trivial H atoms and the methyl groups on the pincer ligand of [Ni]H are omitted for the sake of clarity.

two pathways (starting from [Ni]OOCH + HBcat) involving the six-membered and the four-membered donor−acceptor complex, respectively. Relative to [Ni]OOCH + HBcat, the energies of these transition states are 23.0 kcal/mol (**TSa6**) and 22.6 kcal/mol (**TSa5**). The products of either process, [Ni]H + HCOOBcat, are slightly lower than [Ni]OOCH + HBcat in free energies. These results indicate that both reaction pathways are favorable. HCOOBcat generated via **TSa6** adopts a *cis* conformation (defined based on the relationship between B−O and O═C bonds), which can be easily isomerized to the *trans* conformation by only overcoming a small rotation barrier of 2.4 kcal/mol (**TSa8**). Because the *trans*-HCOOBcat is slightly more stable than its *cis* isomer and they are readily interconverted, we considered only the *trans*-HCOOBcat in the subsequent studies, without specifying its conformation.

Formation of CH_2O. Formaldehyde was not detected in the experiment, but it was proposed to be directly generated from the reaction between HCOOBcat and HBcat. We first examined the direct reaction and considered two possible pathways. The transition states **TSb1** and **TSb2** (shown in Figure 2A) correspond to the attack of HBcat on the C═O double bond and C−O single bond of HCOOBcat, respectively. While **TSb2** leads to CH_2O directly, **TSb1** gives catBOCH$_2$OBcat, which undergoes decomposition to generate CH_2O and catBOBcat. Nevertheless, the predicted barriers of 40.0 kcal/mol (via **TSb1**) and 43.6 kcal/mol (via **TSb2**), relative to 2HBcat + CO_2, are too high to be accessible experimentally at ambient temperature. Therefore, we suspected that [Ni]H might catalyze the formation of CH_2O.

The pathway of [Ni]H-catalyzed formation of CH_2O is shown in Figure 2A. The [Ni]H complex reacts with HCOOBcat, resulting in [Ni]OCH$_2$OBcat, which is decomposed to [Ni]OBcat and CH_2O. The regeneration of [Ni]H is accomplished via the reaction of [Ni]OBcat with HBcat (the second equivalent of HBcat used in a complete catalytic cycle). Analogous to the direct reaction of HCOOBcat with HBcat, as indicated in **TSb1** and **TSb2**, [Ni]H can possibly approach either the C═O or C−O single bond of HCOOBcat. However, the attack on the C−O single bond is highly unlikely, because of the steric clash between HCOOBcat and the bulky ^{t}Bu groups of [Ni]H. Moreover, even in a less sterically crowded situation (see the top of Figure 2A), the interaction between the H−B bond and the C═O double bond (via **TSb1**) is more favorable than the alternative pathway (via **TSb2**) by 3.6 kcal/mol. Therefore, we only need to consider the attack of [Ni]H on the C═O double bond of HCOOBcat. The barrier (**TSb3**) for this step is 32.5 kcal/mol, with respect to [Ni]H + HCOOBcat. The value is substantially lower than that of an uncatalyzed process through either **TSb1** (40.0 kcal/mol) or **TSb2** (43.6 kcal/mol), suggesting the necessity of involving [Ni]H.

The intermediate [Ni]OCH$_2$OBcat is decomposed to CH_2O and [Ni]OBcat and the decomposition barrier (**TSb4**) of 18.1 kcal/mol is small enough to be experimentally reachable. One of the decomposition products [Ni]OBcat further reacts with HBcat to

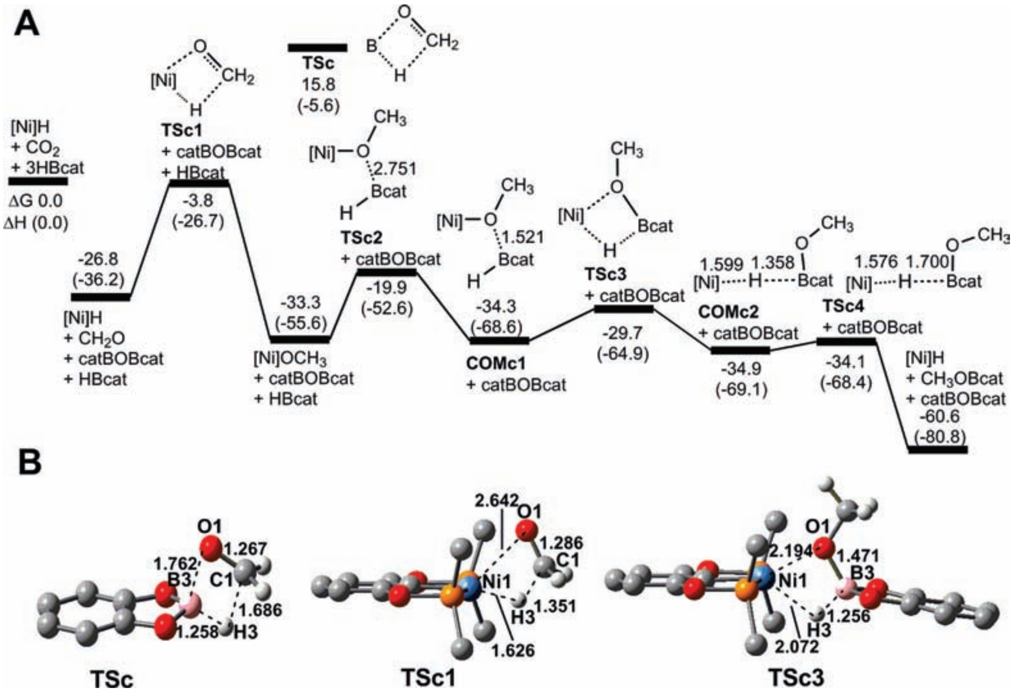

Figure 3. (A) Free-energy profile for CH_3OBcat formation steps (values in kcal/mol; the enthalpy values are listed in the parentheses). The key bond lengths labeled in the stationary points are given in Ångstroms. (B) Optimized structures of important stationary points with key bond lengths (given in Ångstroms). Other optimized structures are given in section SI2 in the Supporting Information. Trivial H atoms and the methyl groups on the pincer ligand of [Ni]H are omitted for the sake of clarity.

reform the [Ni]H catalyst. The reaction of [Ni]OBcat with HBcat gives a donor−acceptor complex **COMb1** after crossing the transition state **TSb5** ($\Delta G^{\ddagger}$ = 21.4 kcal/mol, relative to HBcat + [Ni]OBcat). Following another transition state **TSb6**, the $H^{\delta-}$ of HBcat is transferred to the Ni center with the concurrent cleavage of the Ni−O bond of [Ni]OBcat. The barrier for $H^{\delta-}$ transfer is merely 3.1 kcal/mol, relative to **COMb1**. The resulting H-bridged complex **COMb2** undergoes dissociation to give [Ni]H and catBOBcat, crossing a small barrier of 7.0 kcal/mol (via **TSb7**). The borate ester catBOBcat is one of two final products of the overall catalytic reaction.

Up to this point, the highest stationary point (**TSb3**) for the reduction process is 27.6 kcal/mol higher than that of the reactants ([Ni]H + CO_2 + HBcat). Compared to the ambient conditions used in the experiment, this value is somewhat high. However, it should be noted that the ideal gas phase model inevitably overestimates the entropic contribution for a reaction in a solvent medium.[21] Accurate prediction of enthalpies and entropies in solution remains a challenge for computational chemists and no standard approach is currently available.[22] Nevertheless, in a study of the solvention free energy of aqueous ferric ion, Martin et al.[23a] have proposed to correct the overestimation of entropic contributions by artificially elevating the reaction pressure from 1 atm to 1354 atm. This method was then extended to the studies of the solvation free energies of heavy transition-metal ions.[23b,c] According to the approach, a free-energy correction of 4.3 kcal/mol is applied to the per component change for a reaction at 298.15 K and 1 atm (i.e., a reaction from *m*- to *n*-components has a free-energy correction of $(n - m) \times 4.3$ kcal/mol). If such a correction is employed, the barrier to **TSb3** is 19.0 kcal/mol higher than that of [Ni]H + CO_2 + HBcat in free energy, which is in agreement with the ambient experimental conditions for the catalytic conversion.

The mechanism for CH_2O production (Figure 2A) is quite similar to what has been predicted in the NHC/CO_2/silane system. The [Si]OCH_2O[Si] species in NHC/CO_2/silane system is related to [Ni]OCH_2OBcat in the current system. Although [Ni]OCH_2OBcat was not experimentally detected, its formation from [Ni]H and HCOOBcat is demonstrated here to be energetically feasible. In addition, there are several precedents in the literature for related transition-metal complexes. For instance, Berger et al. have provided spectroscopic evidence of [Zr]OCH_2O[Zr] in the stoichiometric reaction of Cp_2Zr(H)Cl ([Zr]H) with CO_2.[24] Rankin and Cummins have also detected [Ta]OCH_2O[Ta] in their recent investigation of the stoichiometric reaction between $(Ar[{}^tBuCH_2]N)_2(\eta^2\text{-}{}^tBu(H)\text{-}CNAr)TaH$ ([Ta]H) and CO_2.[2c] The proposed [Ni]OCH_2O-Bcat species in the nickel pincer system is probably converted so rapidly to CH_2O and [Ni]OBcat that it cannot be directly observed with common spectroscopic methods. In contrast, the [Si]OCH_2O[Si] species in the NHC/CO_2/silane system was captured by GC-MS.[11] The difference between these two systems is due to the kinetic barriers for the decompostion of the bridging methylene diolate complexes. The calculated barrier for [Si]OCH_2O[Si] decomposition (26.2 kcal/mol) is 8.1 kcal/mol higher than the barrier for [Ni]OCH_2OBcat decomposition. This result confirms that [Ni]OCH_2OBcat is much less persistent than [Si]OCH_2O[Si] in the NHC/CO_2/silane system. Similarly, intermediate [Ni]OBcat in Figure 2A is also short-lived, as the barrier for the reaction of [Ni]OBcat with HBcat is relatively low (21.4 kcal/mol via **TSb5**). Furthermore, the decomposition of [Ni]OCH_2OBcat and the reaction of [Ni]OBcat with HBcat are exoergic by 13.1 and 10.2 kcal/mol, which provide the thermodynamic sink and contribute to the difficulty of detecting these species.

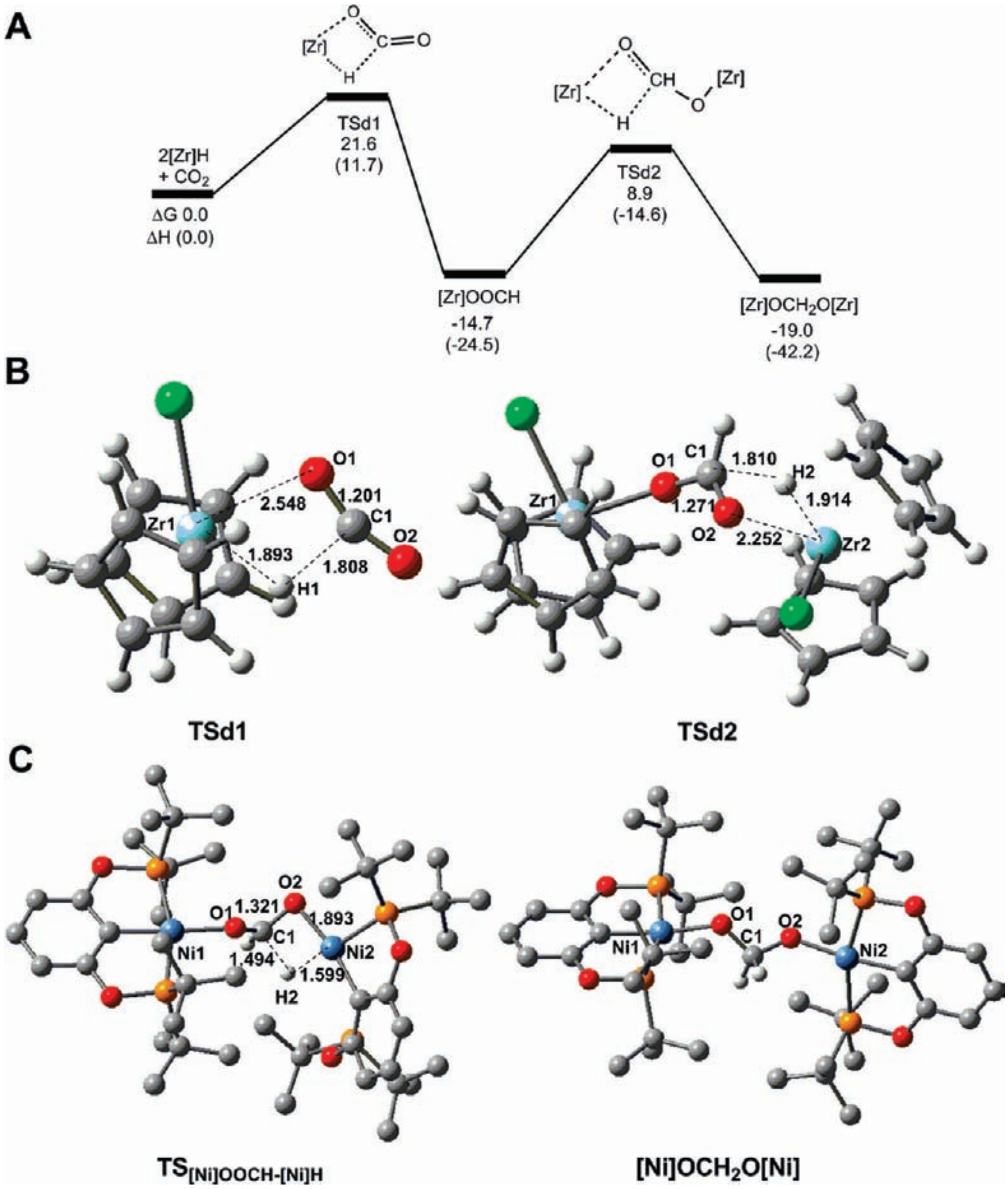

Figure 4. (A) Free-energy profile of the [Zr]H/CO_2 system (values in kcal/mol; enthalpy values are listed in the parentheses). (B) Optimized structures of important stationary points in the [Zr]H/CO_2 system with key bond lengths (given in Ångstroms). Other optimized structures are given in section SI2 in the Supporting Information. (C) Optimized structures of the transition state (left) and the product (right) for the reaction of [Ni]OOCH with [Ni]H. Trivial H atoms on the pincer ligand of [Ni]H are omitted for the sake of clarity.

Formation of CH_3OBcat. CH_3OBcat is the other final product of CO_2 reduction. As shown in Figure 3A, the formation of CH_3OBcat starts with the insertion of CH_2O into the Ni−H bond, which is similar to CO_2 and HCOOBcat insertions (see Figure 1A and 2A). The reaction of CH_2O overcomes the transition state **TSc1** ($\Delta G^{\ddagger} = 23.0$ kcal/mol) to afford [Ni]OCH_3. The latter species interacts with HBcat (the third equivalent of HBcat used in a complete catalytic cycle) to give the donor−acceptor complex **COMc1** after crossing the barrier over **TSc2** ($\Delta G^{\ddagger} = 13.4$ kcal/mol). The four-membered transition state **TSc3** (4.6 kcal/mol) results in the transfer of $H^{\delta-}$ from HBcat to the Ni center of [Ni]OCH_3, providing the H-bridged complex **COMc2**. The dissociation of this complex gives CH_3OBcat and the [Ni]H catalyst by passing a very low barrier of 0.8 kcal/mol (via **TSc4**). The energy profile in Figure 3A suggests that the reduction of CH_2O is energetically favorable; the highest barrier (**TSc1**) in the entire process is 23.0 kcal/mol. Because of the low barrier (13.4 kcal/mol) for the reaction of [Ni]OCH_3 with HBcat, the direct observation of [Ni]OCH_3 is expected to be challenging. The above-mentioned hydroboration of CH_2O promoted by [Ni]H has been indirectly tested by experiments.[12] To avoid the complication of water in commercially available formaldehyde solution, paraformaldehyde was used instead as the substrate to react with [Ni]H. The insertion reaction was sluggish at room temperature, limited by the slow release of CH_2O from paraformaldehyde. Once the nickel alkoxide was formed, its subsequent reaction with HBcat proved to be fast at room temperature.

3.2. Catalytic Effect of [Ni]H.

The computational studies show that each of the three reaction segments involves the transfer of $H^{\delta-}$ from [Ni]H to the carbon atom of CO_2, HCOOBcat, or CH_2O via an insertion reaction (see **TSa1**, **TSb3**, and **TSc1**). Alternatively, HBcat is capable of transferring $H^{\delta-}$ directly to these compounds. To understand the catalytic effect of [Ni]H, the uncatalyzed reactions of HBcat with CO_2, HCOOBcat, and CH_2O were also studied. As compared in Figures 1A−3A, the $H^{\delta-}$ transfer from [Ni]H complex is much more favorable than the direct $H^{\delta-}$ transfer from HBcat; **TSa1**, **TSb3**, and **TSc1** are 30.1, 12.4, and 19.6 kcal/mol lower than **TSa** (Figure 1A), **TSb1** (Figure 2A), and **TSc** (Figure 3A), respectively. The more facile $H^{\delta-}$ transfer from [Ni]H reflects the more-negative $H^{\delta-}$ of the Ni−H bond ($Q = -0.135\ e$) than that of the B−H bond in HBcat ($Q = -0.076\ e$) and the weaker Ni−H bond (WBI = 0.680) than B−H bond (WBI = 0.970).

It has been reported that the reaction of $Cp_2Zr(H)Cl$ ([Zr]H) with CO_2 yields $[Zr]OCH_2O[Zr]$ (and eventual $[Zr]OCH_3$),[4g,h,24] and the reaction of $(Ar[^{t}BuCH_2]N)_2(\eta^2\text{-}^{t}Bu(H)CNAr)TaH$ ([Ta]H) complex with CO_2 leads to $[Ta]OCH_2O[Ta]$.[2c] In principle, a stoichiometric reaction of [Ni]H with CO_2 could also give rise to a complex with CH_2O bridging two nickel centers. Such a species may play an important role in the $[Ni]H/CO_2/HBcat$ catalytic cycle. However, this dinickel species was never observed experimentally. This prompted us to ask the following question: What makes these metal hydride systems so different in the reactivity? Using the reaction of [Zr]H with CO_2 as a representative example, we studied the free-energy profile (Figure 4A) assuming that the reaction goes through an intermediate [Zr]OOCH (similar to [Ni]OOCH in Figure 1A).[25] Interestingly, neither the barrier for CO_2 insertion (21.6 kcal/mol) nor the barrier for the reaction of [Zr]OOCH with [Zr]H (23.6 kcal/mol) is high. The dizirconium species $[Zr]OCH_2O[Zr]$ is 19.0 kcal/mol lower than $CO_2 + 2[Zr]H$. In strong contrast, the reaction $[Ni]OOCH + [Ni]H \rightarrow [Ni]OCH_2O[Ni]$ is extremely unfavorable, both kinetically and thermodynamically; the barrier for the reaction is 62.7 kcal/mol and the reaction is endoergic by 42.8 kcal/mol. Consistent with the calculations, when equimolar amounts of [Ni]H and [Ni]OOCH were mixed in toluene at room temperature or 60 °C, no new species was observed.[20] The significant reactivity difference between [Ni]H and [Zr]H can be attributed to both steric and electronic effects. As demonstrated by the optimized structures in Figure 4C, there is severe steric repulsion between two approaching nickel pincer complexes. In the transition state, one of the $P^{t}Bu_2$ arms must dissociate from the nickel center. In addition, the higher oxyphilicity of the early transition metals (i.e., Zr) may contribute to their unique reaction patterns. In an attempt to separate the steric effect from the overall effects, we replaced the four ^{t}Bu groups in [Ni]H with four Me groups in our calculations. The new $[Ni]OCH_2O[Ni]$ is still 26.9 kcal/mol higher in energy than its corresponding reactants; however, this value is significantly less than 42.8 kcal/mol, corresponding to the original $[Ni]OCH_2O[Ni]$. While [Ni]H does not react with [Ni]OOCH, HBcat is able to react with the [Ni]OOCH, thereby completing the catalytic transformation according to the pathways predicted in Figures 1A−3A. [Zr]H and [Ta]H hydride complexes have the proper and electronic structures to allow them to react with [Zr]OOCH and [Ta]OOCH to give complex $[Zr]OCH_2O[Zr]$ and $[Ta]OCH_2O[Ta]$, respectively. However, breaking the strong Zr−O and Ta−O bonds is expected to be too difficult to close a potential catalytic cycle. Finally, the M06 method,[26,27] which gives a better description of noncovalent interactions than B3LYP method, was employed to further study the reaction $[Ni]OOCH + [Ni]H \rightarrow [Ni]OCH_2O[Ni]$. The high barrier (45.8 kcal/mol) and endogonicity (42.8 kcal/mol) once again verify the difficulty of the reaction.

Scheme 3. The $H^{\delta-}$ Transfer Mechanism with [Ni]H (Mode A) and Direct $H^{\delta-}$ Transfer Mechanism with NHC (Modes B and C)[a]

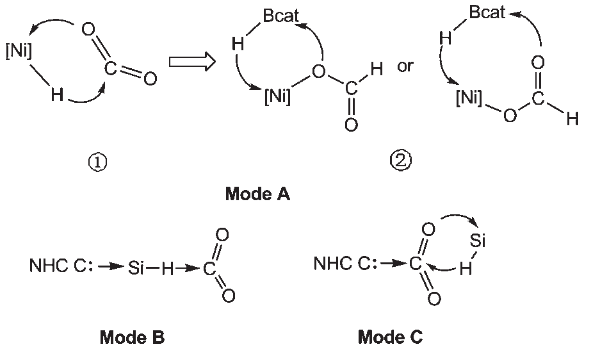

[a] Segments ① and ② are described in the text.

3.3. Catalytic Roles of [Ni]H and NHC: Similarities and Differences.

The NHC/CO_2/silane and $[Ni]H/CO_2/HBcat$ systems are prototypical examples of CO_2 reduction catalyzed by organic compounds and transition-metal complexes, respectively. For the deeper understanding of this important transformation, it is imperative to compare the roles of the two catalytic systems. Both systems feature three $H^{\delta-}$ transfer steps; therefore, 3 equiv of hydrogen sources are needed to reduce 1 equiv of CO_2. The overall function of the catalysts is to facilitate the transfer of $H^{\delta-}$ from the hydrogen source (HBcat or silane) to $CO_2/HCOOBcat/CH_2O$ in the $[Ni]H/CO_2/HBcat$ system or to $CO_2/HCOO[Si]/CH_2O$ in the NHC/CO_2/silane system. How the two catalysts promote the $H^{\delta-}$ transfer is, however, completely different. We use the first $H^{\delta-}$ transfer step as an example to illustrate the differences. In the [Ni]H case, $H^{\delta-}$ transfer is achieved through two sequential steps (Mode A in Scheme 3): in ①, the [Ni]H catalyst first transfers its own $H^{\delta-}$ to CO_2 to generate [Ni]OOCH, and in ②, the nickel complex receives $H^{\delta-}$ from HBcat to reform [Ni]H and release HCOOBcat. The integrity of the catalyst structure changes during catalysis (see Figures 1A−3A). In comparison, the NHC catalyst either activates the silane via Mode B or facilitates the direct $H^{\delta-}$ transfer from silane to an activated CO_2 via Mode C (Scheme 3). In the $H^{\delta-}$ transfer process, the NHC catalyst simply exerts electronic influence to promote the reaction but never gains or loses an H atom. In other words, the integrity of the NHC catalyst structure never changes during catalysis. As a result of direct $H^{\delta-}$ transfer from the silane, there are no intermediates that are equivalent to [Ni]OOCH, $[Ni]OCH_2OBcat$, and $[Ni]OCH_3$ in the NHC/CO_2/silane system. This also explains that, in the NHC/CO_2/silane system, the intermediate after the second $H^{\delta-}$ transfer step is $[Si]OCH_2O[Si]$, with no involvement of the catalyst. In the $[Ni]H/CO_2/HBcat$ system, the intermediate after the second $H^{\delta-}$ transfer step is $[Ni]OCH_2OBcat$ with nickel catalyst incorporated, rather than $catBOCH_2OBcat$, as one might have imagined. The experimentally detected species including HCOOBcat, catBOBcat, and CH_3OBcat are generated from the corresponding nickel species ([Ni]OOCH, [Ni]OBcat, and $[Ni]OCH_3$) and HBcat; they also correlate to the observed HCOO[Si], [Si]O[Si], and $CH_3O[Si]$ in the NHC/CO_2/silane system.

Both catalytic systems use an external hydrogen source to provide $H^{\delta-}$. We were curious to see if the hydrogen sources of the two systems can be switched. To answer this question, we considered the energetics of the first $H^{\delta-}$ transfer step in the two

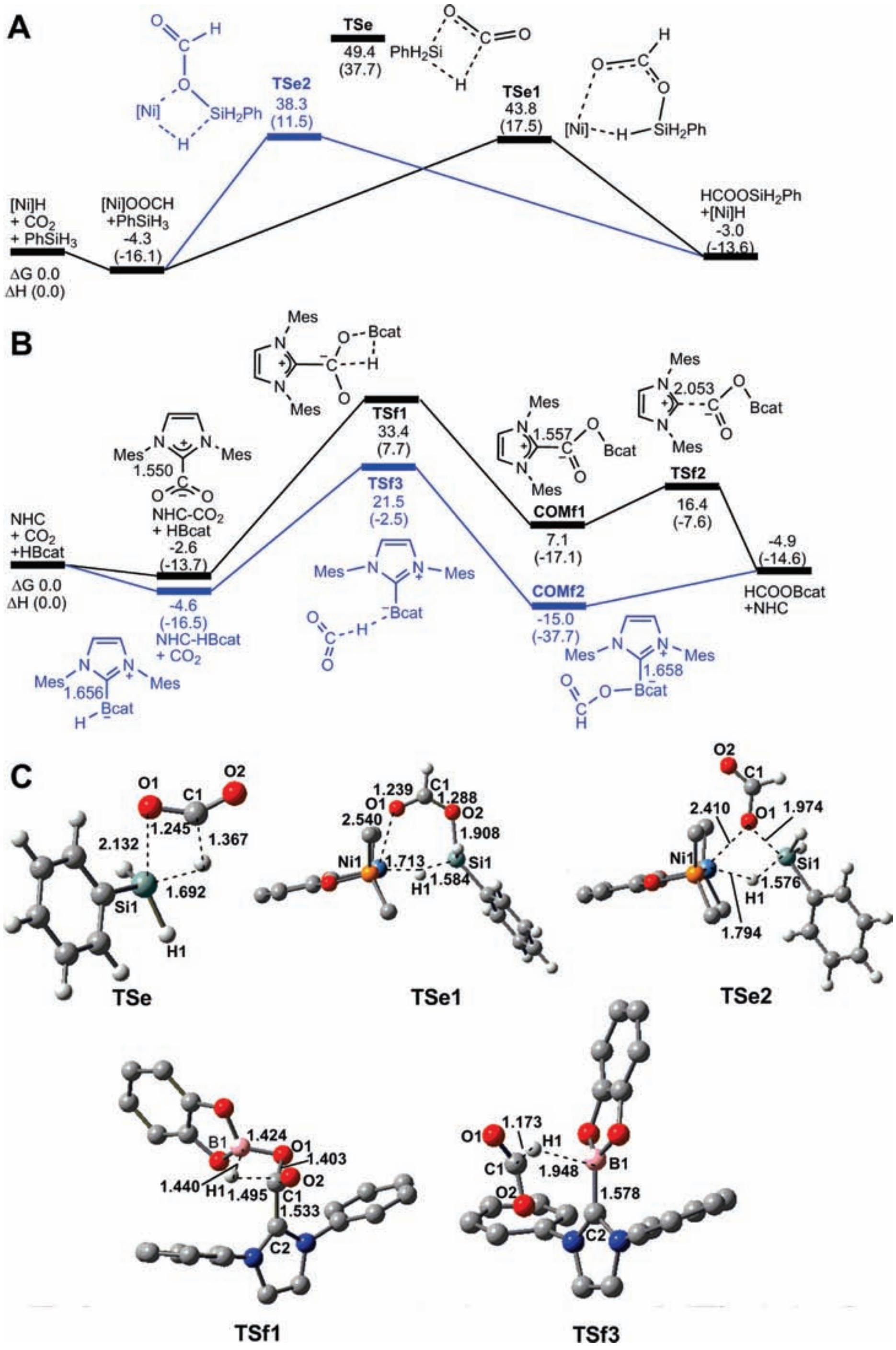

Figure 5. Free-energy profiles of (A) the [Ni]H/CO_2/$PhSiH_3$ system and (B) the NHC/CO_2/HBcat system. (Values are given in kcal/mol; the enthalpy values are listed in the parentheses. The key bond lengths in the stationary points are given in Ångstroms.) (C) Optimized structures of important stationary points with key bond lengths (values shown in black, given in Ångstroms). Other optimized structures are given in section SI2 in the Supporting Information. Trivial H atoms, the methyl groups on the pincer ligand of [Ni]H, and the methyl groups on the mesityl rings of NHC are omitted for the sake of clarity.

systems termed as [Ni]H/CO_2/$PhSiH_3$ and NHC/CO_2/HBcat. The results are summarized in Figure 5.

Without the participation of [Ni]H, the direct reaction of $PhSiH_3$ with CO_2 has a barrier of 49.4 kcal/mol (via **TSe**), which is about the same as that over **TSa** ($\Delta G^{\ddagger}$ = 49.1 kcal/mol; see Figure 1) for the direct reaction of HBcat with CO_2. The small difference in these barriers implies that $PhSiH_3$ and HBcat have comparable $H^{\delta-}$ donor ability. However, the catalytic influence of [Ni]H in [Ni]H/CO_2/$PhSiH_3$ system is not as effective as that in the [Ni]H/CO_2/HBcat system. The relative energies of the six-membered and four-membered transition states (48.1 kcal/mol for **TSe1** and 42.6 kcal/mol for **TSe2**) are much higher than the values of the corresponding transition states in the [Ni]H/CO_2/HBcat system (19.8 kcal/mol for **TSa4** and 22.6 kcal/mol for **TSa5**). The energetic differences can be rationalized by comparing the chemical bonding in the transition states. The

Scheme 4. A Complete Catalytic Cycle of [Ni]H-Catalyzed Reduction of CO_2 to CH_3OBcat^a

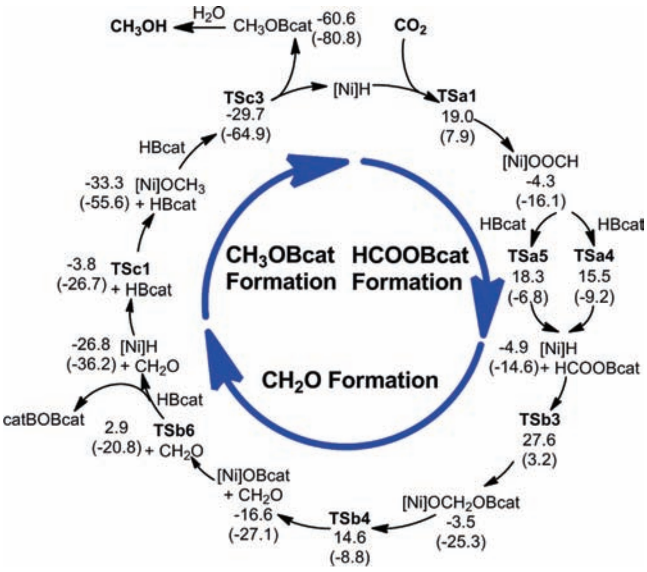

[a] For the sake of clarity, trivial stationary points are not included.

formation of the O2−Si1 (**TSe1**) or O1−Si1 (in **TSe2**) bond distorts the tetrahedral geometry at the Si center and results in a pentacoordinated Si center, which pays a significantly high reorganization energy.[28] In contrast, the O2 atom in **TSa4** or the O1 atom in **TSa5** interacts favorably with an electron-deficient B atom via a donor−acceptor interaction. Note that the barriers for other silanes may vary greatly; however, the general conclusion that silanes are not as good as HBcat to serve as the hydrogen sources in [Ni]H-catalyzed CO_2 reduction holds true. Indeed, no reaction was observed when [Ni]OOCH was mixed with 1 equiv of $PhSiH_3$ at room temperature for one day.[20] Attempted catalytic hydrosilylation of CO_2 with $PhSiH_3$ in the presence of 1 mol % of [Ni]H did not yield any reduction products.

In the NHC/CO_2/HBcat system, the two barriers (33.4 kcal/mol for **TSf1** and 21.5 kcal/mol for **TSf3**) of $H^{\delta-}$ transfer via the two different activation modes (Modes C and B in Scheme 3) are not high for experimental realization. However, the liberation of NHC catalyst in the mode B activation pathway can be problematic, because **COMf2** is too stable (10.1 kcal/mol more stable than HCOOBcat + NHC). Our previous study of the NHC/CO_2/silane system has shown that NHC is very easily released and the intermediate analogous to **COMf2** is even less stable than NHC + HCOO[Si]. Therefore, HBcat may not be a good hydrogen source for NHC-catalyzed CO_2 reduction. Note that the problem of releasing NHC could be circumvented through the use of a sterically more demanding NHC. Further experiments are needed to test this hypothesis.

4. CONCLUSIONS

Our computational mechanistic study has elucidated how [Ni]H facilitates the catalytic conversion of CO_2 to a methanol derivative. As shown in the complete catalytic cycle (Scheme 4), the overall transformation involves three $H^{\delta-}$ transfer steps and [Ni]H participates in each one of them. The catalytic role of [Ni]H is to shuttle $H^{\delta-}$ from HBcat to CO_2, HCOOBcat, and CH_2O. The direct reaction of HBcat with CO_2 is highly unfavorable. The predicted intermediates [Ni]OCH_2OBcat, [Ni]OBcat, and [Ni]OCH_3 could be fleeting species, because of the facile decomposition of [Ni]OCH_2OBcat and low barriers for the reactions of [Ni]OBcat and [Ni]OCH_3 with HBcat. In comparison, the NHC catalyst in the NHC/CO_2/silane system facilitates the direct $H^{\delta-}$ transfer from silane to CO_2, HCOO-[Si], and CH_2O. The integrity of the catalyst structure never changes during the entire process. Switching the hydrogen sources in the two catalytic systems results in less-favorable reactions. The [Ni]H/CO_2/$PhSiH_3$ system has a high kinetic barrier for the reaction between [Ni]OOCH and $PhSiH_3$, while the NHC/CO_2/HBcat system has a thermodynamically stable intermediate (NHC-HCOOBcat) that makes the release of NHC problematic. The present study has demonstrated that, depending on the reaction mechanism, the CO_2 reduction catalyst should be matched with an appropriate hydrogen source.

■ ASSOCIATED CONTENT

Ⓢ Supporting Information. This material is available free of charge via the Internet at http://pubs.acs.org.

■ AUTHOR INFORMATION

Corresponding Author

*E-mails: zxwang@gucas.ac.cn (Z.-X.W.), hairong.guan@uc.edu (H.G.).

■ ACKNOWLEDGMENT

This work is financially supported by funds from the Chinese Academy of Sciences, the National Natural Science Foundation of China (Nos. 20973197 and 20773160, to Z.-X.W.), and the U. S. National Science Foundation (No. CHE-0952083, to H.G.).

■ REFERENCES

(1) For recent reviews on CO_2 transformation, see:(a) Kember, M. R.; Buchard, A.; Williams, C. K. *Chem. Commun.* **2011**, *47*, 141. (b) Darensbourg, D. J. *Inorg. Chem.* **2010**, *49*, 10765. (c) Riduan, S. N.; Zhang, Y. *Dalton Trans.* **2010**, *39*, 3347. (d) Mikkelsen, M.; Jørgensen, M.; Krebs, F. C. *Energy Environ. Sci.* **2010**, *3*, 43. (e) Sakakura, T.; Kohno, K. *Chem. Commun.* **2009**, 1312. (f) Olah, G. A.; Goeppert, A.; Prakash, G. K. S. *J. Org. Chem.* **2009**, *74*, 487. (g) Correa, A.; Martín, R. *Angew. Chem., Int. Ed.* **2009**, *48*, 6201. (h) Yu, K. M. K.; Curcic, I.; Gabriel, J.; Tsang, S. C. E. *ChemSusChem* **2008**, *1*, 893. (i) Sakakura, T.; Choi, J. -C.; Yasuda, H. *Chem. Rev.* **2007**, *107*, 2365. (j) Darensbourg, D. J. *Chem. Rev.* **2007**, *107*, 2388. (k) Aresta, M.; Dibenedetto, A. *Dalton Trans.* **2007**, 2975. (l) Olah, G. A. *Angew. Chem., Int. Ed.* **2005**, *44*, 2636. (m) Coates, G. W.; Moore, D. R. *Angew. Chem., Int. Ed.* **2004**, *43*, 6618.

(2) For recent reports on CO_2 fixation, see:(a) Buchard, A.; Kember, M. R.; Sandeman, K. G.; Williams, C. K. *Chem. Commun.* **2011**, *47*, 212. (b) Ren, W.-M.; Zhang, X.; Liu, Y.; Li, J.-F.; Wang, H.; Lu, X.-B. *Macromolecules* **2010**, *43*, 1396. (c) Rankin, M. A.; Cummins, C. C. *J. Am. Chem. Soc.* **2010**, *132*, 10021. (d) Langer, J.; Imhof, W.; Fabra, M. J.; García-Orduña, P.; Görls, H.; Lahoz, F. J.; Oro, L. A.; Westerhausen, M. *Organometallics* **2010**, *29*, 1642. (e) Kember, M. R.; White, A. J. P.; Williams, C. K. *Macromolecules* **2010**, *43*, 2291. (f) He, C.; Tian, G.; Liu, Z.; Feng, S. *Org. Lett.* **2010**, *12*, 649. (g) Decortes, A.; Belmonte, M. M.; Benet-Buchholz, J.; Kleij, A. W. *Chem. Commun.* **2010**, *46*, 4580. (h) Clegg, W.; Harrington, R. W.; North, M.; Pasquale, R. *Chem.—Eur. J.* **2010**, *16*, 6828. (i) Mömming, C. M.; Otten, E.; Kehr, G.; Fröhlich, R.; Grimme, S.; Stephan, D. W.; Erker, G. *Angew. Chem., Int. Ed.* **2009**, *48*, 6643. (j) Kember, M. R.; White, A. J. P.; Williams, C. K.

Inorg. Chem. **2009**, *48*, 9535. (k) Kember, M. R.; Knight, P. D.; Reung, P. T. R.; Williams, C. K. *Angew. Chem., Int. Ed.* **2009**, *48*, 931. (l) Kayaki, Y.; Yamamoto, M.; Ikariya, T. *Angew. Chem., Int. Ed.* **2009**, *48*, 4194. (m) Dang, L.; Lin, Z.; Marder, T. B. *Organometallics* **2010**, *29*, 917. (n) Li, J.; Jia, G.; Lin, Z. *Organometallics* **2008**, *27*, 3892.

(3) (a) Berkefeld, A.; Piers, W. E.; Parvez, M. *J. Am. Chem. Soc.* **2010**, *132*, 10660. (b) Matsuo, T.; Kawaguchi, H. *J. Am. Chem. Soc.* **2006**, *128*, 12362.

(4) (a) Roy, L.; Zimmerman, P. M.; Paul, A. *Chem.—Eur. J.* **2011**, *17*, 435. (b) Ménard, G.; Stephan, D. W. *J. Am. Chem. Soc.* **2010**, *132*, 1796. (c) Ashley, A. E.; Thompson, A. L.; O'Hare, D. *Angew. Chem., Int. Ed.* **2009**, *48*, 9839. (d) Chan, B.; Radom, L. *J. Am. Chem. Soc.* **2008**, *130*, 9790. (e) Chan, B.; Radom, L. *J. Am. Chem. Soc.* **2006**, *128*, 5322. (f) Tominaga, K.; Sasaki, Y.; Kawai, M.; Watanabe, T.; Saito, M. *J. Chem. Soc.—Chem. Commun.* **1993**, 629. (g) Gambarotta, S.; Strologo, S.; Floriani, C.; Chiesi-Villa, A.; Guastini, C. *J. Am. Chem. Soc.* **1985**, *107*, 6278. (h) Fachinetti, G.; Floriani, C.; Roselli, A.; Pucci, S. *J. Chem. Soc.—Chem. Commun.* **1978**, 269. (i) Eisenschmid, T. C.; Eisenberg, R. *Organometallics* **1989**, *8*, 1822.

(5) For representative reviews on the conversion of CO_2 to HCOOH, see:(a) Jessop, P. G.; Joó, F.; Tai, C. C. *Coord. Chem. Rev.* **2004**, *248*, 2425. (b) Leitner, W. *Angew. Chem., Int. Ed.* **1995**, *34*, 2207. (c) Jessop, P. G.; Ikariya, T.; Noyori, R. *Chem. Rev.* **1995**, *95*, 259.

(6) For recent experimental studies on the conversion of CO_2 to HCOOH, see:(a) Sanz, S.; Benítez, M.; Peris, E. *Organometallics* **2010**, *29*, 275. (b) Federsel, C.; Jackstell, R.; Beller, M. *Angew. Chem., Int. Ed.* **2010**, *49*, 6254. (c) Federsel, C.; Boddien, A.; Jackstell, R.; Jennerjahn, R.; Dyson, P. J.; Scopelliti, R.; Laurenczy, G.; Beller, M. *Angew. Chem., Int. Ed.* **2010**, *49*, 9777. (d) Zhang, Z.; Hu, S.; Song, J.; Li, W.; Yang, G.; Han, B. *ChemSusChem* **2009**, *2*, 234. (e) Tanaka, R.; Yamashita, M.; Nozaki, K. *J. Am. Chem. Soc.* **2009**, *131*, 14168. (f) Zhang, Z.; Xie, Y.; Li, W.; Hu, S.; Song, J.; Jiang, T.; Han, B. *Angew. Chem., Int. Ed.* **2008**, *47*, 1127. (g) Himeda, Y. *Eur. J. Inorg. Chem.* **2007**, 3927.

(7) For recent theoretical studies on the conversion of CO_2 to HCOOH, see:(a) Ahlquist, M. S. G. *J. Mol. Catal. A-Chem.* **2010**, *324*, 3. (b) Getty, A. D.; Tai, C. -C.; Linehan, J. C.; Jessop, P. G.; Olmstead, M. M.; Rheingold, A. L. *Organometallics* **2009**, *28*, 5466. (c) Urakawa, A.; Jutz, F.; Laurenczy, G.; Baiker, A. *Chem.—Eur. J.* **2007**, *13*, 3886. (d) Huang, K. -W.; Han, J. H.; Musgrave, C. B.; Fujita, E. *Organometallics* **2007**, *26*, 508. (e) Ohnishi, Y.; Nakao, Y.; Sato, H.; Sakaki, S. *Organometallics* **2006**, *25*, 3352. (f) Ogo, S.; Kabe, R.; Hayashi, H.; Harada, R.; Fukuzumi, S. *Dalton Trans.* **2006**, 4657. (g) Ohnishi, Y.; Matsunaga, T.; Nakao, Y.; Sato, H.; Sakaki, S. *J. Am. Chem. Soc.* **2005**, *127*, 4021.

(8) For experimental studies on CO_2 cleavage, see:(a) Silvia, J. S.; Cummins, C. C. *J. Am. Chem. Soc.* **2010**, *132*, 2169. (b) Gu, L.; Zhang, Y. *J. Am. Chem. Soc.* **2010**, *132*, 914. (c) van der Boom, M. E. *Angew. Chem., Int. Ed.* **2009**, *48*, 28. (d) Whited, M. T.; Grubbs, R. H. *J. Am. Chem. Soc.* **2008**, *130*, 5874. (e) Sadique, A. R.; Brennessel, W. W.; Holland, P. L. *Inorg. Chem.* **2008**, *47*, 784. (f) Allen, O. R.; Dalgarno, S. J.; Field, L. D. *Organometallics* **2008**, *27*, 3328. (g) Laitar, D. S.; Müller, P.; Sadighi, J. P. *J. Am. Chem. Soc.* **2005**, *127*, 17196.

(9) For theoretical studies on CO_2 cleavage, see:(a) Brookes, N. J.; Ariafard, A.; Stranger, R.; Yates, B. F. *J. Am. Chem. Soc.* **2009**, *131*, 5800. (b) Zhao, H.; Lin, Z.; Marder, T. B. *J. Am. Chem. Soc.* **2006**, *128*, 15637. (c) Li, J.; Lin, Z. *Organometallics* **2009**, *28*, 4231.

(10) Ford, P. C.; Trabuco, E.; Mdleleni, M. M., . In *Encyclopedia of Catalysis*, 1st ed; Horváth, I. T., Ed.; Wiley Interscience: Hoboken, NJ, 2003; Vol. 6, pp 651.

(11) Riduan, S. N.; Zhang, Y.; Ying, J. Y. *Angew. Chem., Int. Ed.* **2009**, *48*, 3322.

(12) Chakraborty, S.; Zhang, J.; Krause, J. A.; Guan, H. *J. Am. Chem. Soc.* **2010**, *132*, 8872.

(13) Huang, F.; Lu, G.; Zhao, L.; Li, H.; Wang, Z.-X. *J. Am. Chem. Soc.* **2010**, *132*, 12388.

(14) (a) Stephens, P. J.; Devlin, F. J.; Chabalowski, C. F.; Frisch, M. J. *J. Phys. Chem.* **1994**, *98*, 11623. (b) Becke, A. D. *J. Chem. Phys.* **1993**, *98*, 5648. (c) Lee, C.; Yang, W.; Parr, R. G. *Phys. Rev. B* **1988**, *37*, 785.

(15) (a) Wadt, W. R.; Hay, P. J. *J. Chem. Phys.* **1985**, *82*, 284. (b) Hay, P. J.; Wadt, W. R. *J. Chem. Phys.* **1985**, *82*, 270. (c) Hay, P. J.; Wadt, W. R. *J. Chem. Phys.* **1985**, *82*, 299.

(16) (a) Sang-Aroon, W.; Ruangpornvisuti, V. *Int. J. Quantum Chem.* **2008**, *108*, 1181. (b) Tomasi, J.; Mennucci, B.; Cances, E. *J. Mol. Struct. Theochem.* **1999**, *464*, 211.

(17) (a) Carpenter, J. E.; Weinhold, F. *J. Mol. Struct. Theochem.* **1988**, *46*, 41. (b) Reed, A. E.; Weinhold, F. *J. Chem. Phys.* **1983**, *78*, 4066. (c) Foster, J. P.; Weinhold, F. *J. Am. Chem. Soc.* **1980**, *102*, 7211.(d) Glendening, E. D.; Reed, A. E.; Carpenter, J. E.; Weinhold, F. *NBO Version 3.1*.

(18) Frisch, M. J.; et al. *Gaussian 03, revision E.01*; Gaussian, Inc.: Wallingford, CT, 2004. (See the Supporting Information for the complete reference of Gaussian 03.)

(19) Schmeier, T. J.; Hazari, N.; Incarvito, C. D.; Raskatov, J. A. *Chem. Commun.* **2011**, *47*, 1824.

(20) Zhang, J.; Chakraborty, S.; Krause, J. A.; Huang, K.-W.; Guan, H. Unpublished results.

(21) (a) Zhang, C. G.; Zhang, R.; Wang, Z. X.; Zhou, Z.; Zhang, S. B.; Chen, Z. *Chem.—Eur. J.* **2009**, *15*, 5910. (b) Liang, Y.; Liu, S.; Xia, Y.; Li, Y.; Yu, Z. X. *Chem.—Eur. J.* **2008**, *14*, 4361. (c) Chen, Y.; Ye, S.; Jiao, L.; Liang, Y.; Sinha-Mahapatra, D. K.; Herndon, J. W.; Yu, Z. X. *J. Am. Chem. Soc.* **2007**, *129*, 10773. (d) Yu, Z. X.; Houk, K. N. *J. Am. Chem. Soc.* **2003**, *125*, 13825. (e) Strajbl, M.; Sham, Y. Y.; Villà, J.; Chu, Z. T.; Warshel, A. *J. Phys. Chem. B* **2000**, *104*, 4578. (f) Hermans, J.; Wang, L. *J. Am. Chem. Soc.* **1997**, *119*, 2707. (g) Amzel, L. M. *Proteins* **1997**, *28*, 144.

(22) (a) Bennaim, A.; Marcus, Y. *J. Chem. Phys.* **1984**, *81*, 2016. (b) Tissandier, M. D.; Cowen, K. A.; Feng, W. Y.; Gundlach, E.; Cohen, M. H.; Earhart, A. D.; Coe, J. V.; Tuttle, T. R. *J. Phys. Chem. A* **1998**, *102*, 7787. (c) Kelly, C. P.; Cramer, C. J.; Truhlar, D. G. *J. Phys. Chem. B* **2006**, *110*, 16066.

(23) (a) Martin, R. L.; Hay, P. J.; Pratt, L. R. *J. Phys. Chem. A* **1998**, *102*, 3565. (b) Gutowski, K. E.; Dixon, D. A. *J. Phys. Chem. A* **2006**, *110*, 8840. (c) Dinescu, A.; Clark, A. E. *J. Phys. Chem. A* **2008**, *112*, 11198.

(24) (a) Schlörer, N. E.; Cabrita, E. J.; Berger, S. *Angew. Chem., Int. Ed.* **2002**, *41*, 107. (b) Schlörer, N. E.; Berger, S. *Organometallics* **2001**, *20*, 1703.

(25) The structures involved in this pathway were optimized at the B3LYP/BSI level. The energies were obtained at B3LYP level with the basis set 6-31+G** for all atoms except Zr (Lanl2DZ basis set). The experimentally employed solvent THF was used to account for solvent effects.

(26) Zhao, Y.; Truhlar, D. G. *Theor. Chem. Acc.* **2008**, *120*, 215.

(27) The M06 DFT calculations were performed using Gaussian 09. (See Frisch, M. J.; et al. *Gaussian 09, revision A.01*; Gaussian, Inc.: Wallingford, CT, 2009. See the Supporting Information for the complete reference of Gaussian 09.)

(28) The reorganization energy was defined as the energy difference between the free $PhSiH_3$ and the structure similar to the $PhSiH_3$ moiety in transition states **TSe1** and **TSe2**. Accordingly, the reorganization energies were calculated as 32.6 kcal/mol in **TSe1** and 16.2 kcal/mol in **TSe2**.